Available online at www.sciencedirect.com

SCIENCE DIRECT®

International Journal of Heat and Mass Transfer 48 (2005) 3713–3721

International Journal of HEAT and MASS TRANSFER

www.elsevier.com/locate/ijhmt

Thermal model of the MUPUS penetrator

K. Seweryn [a,*], M. Banaszkiewicz [a], M. Grunwald [b], J. Grygorczuk [a], T. Spohn [c]

[a] *Space Research Center, Polish Academy of Science, Ul. Bartycka 18A, 00-716 Warsaw, Poland*
[b] *Institute of Aviation EDC, Al. Krakowska 110/114, 02-256 Warsaw, Poland*
[c] *German Aerospace Center DLR, Rutherford 2, 12489 Berlin, Germany*

Received 25 March 2005

Abstract

The insertion device for the MUPUS penetrator on Phylae, the lander to be set by the Rosetta mission on the nucleus of Tchurumov-Gerasimenko comet, will have to work in extreme environmental condition. The electronic unit inside the device should be kept at the temperature greater than −55 °C (220 K) in order to work properly. The expected temperature of the nucleus is of about 130 K, while the cosmic background temperature is as low as 3 K. Therefore, the electronic box must be heated continuously to balance the heat loss by radiation. The experiments performed in a vacuum-thermal chamber on the flight model of MUPUS has shown that the temperature of the electronics increases, when heated with a power of 1.33 W, from 140 K by about 120–130 K after more than 1 h of heating. We present a numerical thermal (FEM) model that gives a very good fit to the measured temperature dependence on time. In the process of fitting, several important thermal parameters of the insertion device have been determined, for instance the emissivity of electronic boards and their specific heat. The numerical models agree qualitatively with the results of simple thermal analysis. The main conclusion concerning performance of the instrument on the comet is that it should safely operate above the lover limit of acceptable temperatures against expected variations of the external temperature in the day-night cycle of the comet.

Keywords: Radiation; Rosetta; Phylae; MUPUS; FEM

1. Introduction

The ESA cornerstone mission Rosetta to comet Tchurumov-Gerasimenko has been launched in February 2004. The most challenging technical goal of the mission is to send the lander to the comet nucleus. If the landing is successfully performed, the mission is supposed to bring a vast amount of in situ data about nucleus chemical composition and its physical properties. The lander is equipped with a drill and a penetrator to carry out investigations on subsurface layers of the comet. The penetrator itself is a part of the scientific experiment MUPUS (multi-purpose sensors for surface and sub-surface science) that aims at measuring the thermal profile of the cometary material down to a depth of about 40 cm as well as at deriving thermal conductivity of the nucleus and its mechanical strength. In addition to

* Corresponding author. Tel.: +48 22 840 37 66; fax: +48 22 840 31 31.
E-mail address: ksewery n@cbk.waw.pl (K. Seweryn).

0017-9310/$ - see front matter
doi:10.1016/j.ijheatmasstransfer.2005.04.003

Nomenclature

$A = \frac{Q+\int\int_s \mathrm{d}s\cdot\varepsilon\cdot\sigma\cdot T_s^4}{\int\int\int_V \mathrm{d}V\cdot\rho\cdot C_b}$ constants

$B = \frac{\int\int_s \mathrm{d}s\cdot\varepsilon\cdot\sigma}{\int\int\int_V \mathrm{d}V\cdot\rho\cdot C_b}$ constants

$C = \frac{Q+\int\int_s \mathrm{d}s\cdot\varepsilon\cdot\sigma\cdot T_s^4+\left(\int\int_{S_1}\frac{\lambda_1\cdot \mathrm{d}S_1}{l_1}+\int\int_{S_2}\frac{\lambda_2\cdot \mathrm{d}S_2}{l_2}\right)\cdot T_s}{\int\int\int_V \mathrm{d}V\cdot\rho\cdot C_b}$ constants

C_b mean specific heat of the electronic board materials [J/kg K]

$D = \frac{\int\int_{S_1} \mathrm{d}S_1\cdot\frac{\lambda_1}{l_1}+\int\int_{S_2} \mathrm{d}S_2\cdot\frac{\lambda_2}{l_2}}{\int\int\int_V \mathrm{d}V\cdot\rho\cdot C_b}$ constants

l_1, l_2 lengths of harness wires and insulating stand, respectively [m]

Q applied power [W]

s radiating surface [m^2]

S_w isothermal cross-section [m^2]

S_1, S_2 isothermal cross-section [m^2]

spc internal space temperature [K]

V volume of the electronic board [m^3]

t time [min]

T temperature [K]

T_s external temperature [K]

Greek symbols

ε emissivity [–]

λ thermal conductivity [W/m K]

λ_1, λ_2 thermal conductivity of harness wires and insulating stand, respectively [W/m K]

ρ mean density of the electronic board materials [kg/m^3]

σ Stefan–Boltzman constants [W/m^2 K^4]

a penetrator, MUPUS comprises: (i) a thermal mapper that observes the vicinity of the lander in infrared and measures the surface temperature, (ii) an accelerometer and a temperature sensor, both located on the harpoon that will be shoot just after landing and will be able to reach a depth of a few meters.

The penetrator is a very complicated subsystem that should perform many technical and scientific functions after landing. First of all it should be released from the locks that keep it fixed on the lander balcony. Then it should be deployed for about 1 m away from the lander to minimize the thermal influence of the lander on the penetrator measurements. Finally, it should be self inserted into the cometary nucleus. After performing this complex set of operations, the penetrator will be ready to act as a thermal probe. Since the long cables between the probe and the lander exclude the transmission of analog signals, as it would easily get corrupted, one must process and digitize the measurements in the penetrator itself and after that send them to the MUPUS main processing unit. Taking into account that the average temperature on the comet will be 120–150 K and that the electronic elements should not be switched on below 220 K, a system of small heaters is required to keep the electronic boards inside the penetrator unit in relatively warm conditions. Such heaters, in the form of thin copper paths on a kapton foil substrate have been manufactured and fixed to the rear side of the circular boards containing the electrical elements. The power generated in each of the three heaters amounted to 0.45–0.5 W and was about maximum of what was allowed by the strict rules of power sharing among many lander instruments.

The engineering and flight model both underwent a series of environmental tests in a vacuum-thermal chamber. Although the main aim of those tests was to check whether the mechanical functions could be successfully performed in demanding conditions (minimum temperature of 100 K, temperature cycle amplitude of 200 K, and vacuum of about 2.5×10^{-6} mbar), the performance of the PENEL heaters was also tested. The obtained results has shown that with the available power of slightly less than 1.5 W, the interior of the PENEL cup can be heated up to about 270 K when the surrounding environment is at about 100 K. The time needed to reach such a temperature was more than an hour.

An important question is then whether it is possible to describe the obtained thermal characteristics in terms of a solution of the heat transfer equation. The positive answer would not only increase the confidence about our understanding of the instrument performance, but also allow us to predict how the temperature inside the electronic compartment will vary on the comet, in conditions that will be different from what was experienced during vacuum-thermal tests. To obtain such a description one should built a comprehensive thermal model of the instrument and to confront it with the measured temperature variation during heating. Since not all parameters of the model are known accurately, one should perhaps iteratively adjust them by fitting the modeled curve to the experimental one. Such approach is taken in this paper.

The paper is organized as follows. First, we present a set of simple thermal models to find out the overall characteristics of the system: the expected final temperature as a function of applied heating power, the time constant of reaching the steady state, the contribution of heat conduction and heat radiation to the heat balance of the electronic box. In the next section we give a description of the FEM model used and list the parameters employed in modeling. The following section contains the results and their interpretation. Finally, we discuss the thermal characteristics of the modeled unit and point out at possible improvement in its thermal design.

2. Simple analysis

There are two levels of analysis that should be performed before employing a full numerical FEM code. The first one consists in applying basic laws to choose the most important physical processes, to determine the steady state of the system that is reached when the heat source input is balanced by losses due to heat transport, and to find the expected time constant of the heating process. The result of such an approach should give an order of magnitude estimate of the steady state temperature and should indicate how long one should wait to get close to the steady state. Then, those estimates could be confronted with the experimental results on one hand and with the model calculations on the other. Any significant discrepancy between both would indicate that some important physical process was not taken into account or that input parameters of the model were not set correctly.

The second level includes simplifications done for the purpose of a numerical thermal model. For example, there are more than 100 parts in the whole insertion device made from more than 20 different materials. It is not necessary to go to such details in modeling, especially when the parts are small and their physical properties do not differ too much. Moreover, a careful optimization of a computational mesh is required to avoid to large number of finite elements, on one side, and too crude meshing on the other. The first possibility would result in a prohibitive running time of the code; the second could lead to large errors in the computed temperature distribution.

As for the simple models, we start with estimating the time needed to reach the steady state. The electronic part of the insertion unit that is relevant for thermal analysis of the heating process is modeled as cylinder formed from three circular boards, each one equipped with an extended heater attached to the rear side of the board. The time dependent heat balance equation, in which only radiation loss is included, reads:

$$\int\int\int_V \mathrm{d}V \cdot \rho \cdot C_b \cdot \frac{\mathrm{d}T}{\mathrm{d}t} = Q - \int\int_S \mathrm{d}S \cdot \varepsilon \cdot \sigma \cdot (T^4 - T_s^4) \tag{1}$$

Introducing the constants A and B one gets:

$$\frac{\mathrm{d}T}{\mathrm{d}t} = A - B \cdot T^4 \tag{2}$$

In our case the approximate values of constants are $A = 0.039$ and $B = 1.063 \times 10^{-11}$. They have been calculated assuming the following material constants and geometric factors: the mass of the electronic board $M = V\rho = 0.05$ kg, its total surface area $s = 1.5 \times 10^{-2}$ m^2, the average specific heat of the boards $C_b = 800$ J/kg K, and its average emissivity $\varepsilon = 0.5$. The ambient temperature T_s was taken to be 150 K. The most uncertain quantities in the model are the emissivity and specific heat.

This differential equation can be integrated [6]:

$$t = \frac{1}{4} \cdot \left(\frac{A}{B}\right)^{\frac{1}{4}} \cdot \frac{\ln\left[-\frac{T + \left(\frac{A}{B}\right)^{\frac{1}{4}}}{\left[T - \left(\frac{A}{B}\right)^{\frac{1}{4}}\right]}\right] + 2 \cdot \arctan\left[\frac{T}{\left(\frac{A}{B}\right)^{\frac{1}{4}}}\right]}{A} \tag{3}$$

Unfortunately, this formula can be analytically inverted to give the temperature variation with time only when the second term in the numerator is assumed to be constant. Such an approximation gives the steady-state temperature consistent with the numerical result, but diverges at small time. Therefore, we will use the numerical solution of Eq. (2).

The numerical (2) temperature dependence is shown in Fig. 1. One can see that the characteristic time to reach the steady state is about 80 min.

From Fig. 1 one can estimate the final temperature in the steady state. It is about 245 K and is lower by about 20 K then the temperature measured during experiments in the vacuum-thermal chamber. Therefore, one can speculate that a part of energy emitted from the boards returns to them after being reflected from the enclosure If this effect is taken into account, the final temperature obtained from the model will be larger.

On the other hand, there is a counteracting process that leads to energy loss and cooling of the boards: a part of the heat flux escapes through the harness (copper

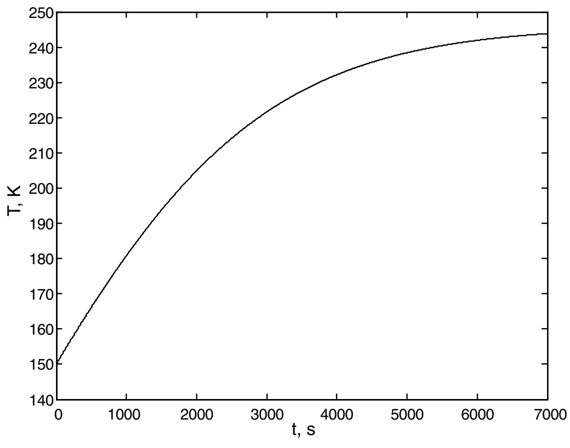

Fig. 1. Numerical solution of the simple model with the source term and radiation loss only.

wires) and the insulating stand. The heat flux, which escapes by thermal conduction, is:

$$q = \lambda \cdot S_w \cdot \mathrm{grad}\,(T) \qquad (4)$$

Approximating the gradient in (4) by temperature difference, grad $(T) \approx (T - T_s)/l_i$, and substituting the thermal conductivity (λ_i), the surface area (S_{wi}), and the length (l_i) of the wire ($i = 1$) and the stand ($i = 2$), one will obtain $q = 0.2$ W for the wire and $q = 0.2$ W for the delrin stand. Those quantities are not negligible; hence Eq. (1) should be completed with a thermal conduction term. The equation, that takes into account the heat loss trough both radiation and conduction, reads:

$$\int\int\int_V \mathrm{d}V \cdot \rho \cdot C_b \cdot \frac{\mathrm{d}T}{\mathrm{d}t} = Q - \int\int_S \mathrm{d}S \cdot \varepsilon \cdot \sigma \cdot (T^4 - T_s^4) - \left(\int\int_{S_1} \frac{\lambda_1 \cdot \mathrm{d}S_1}{l_1} + \int\int_{S_2} \frac{\lambda_2 \cdot \mathrm{d}S_2}{l_2}\right) \cdot (T - T_s) \qquad (5)$$

Introducing the constants C, B and D one gets:

$$\frac{\mathrm{d}T}{\mathrm{d}t} = C - B \cdot T^4 - D \cdot T \qquad (6)$$

The constants C, B, and D can be specified only approximately. Employing the material and geometric factors introduced earlier in this section one obtains: $C = 0.053$, $B = 1.063 \times 10^{-11}$, $D = 9.5 \times 10^{-5}$.

The determination of T from (6) is analytically possible, when an approximation similar to that mentioned above, while discussing the solution of Eq. (3), is used, but the resulting formula depends on the values of different roots of a fourth order algebraic equation, hence is very long and complicated. In Fig. 2, we present only the numerical (6) temperature dependence.

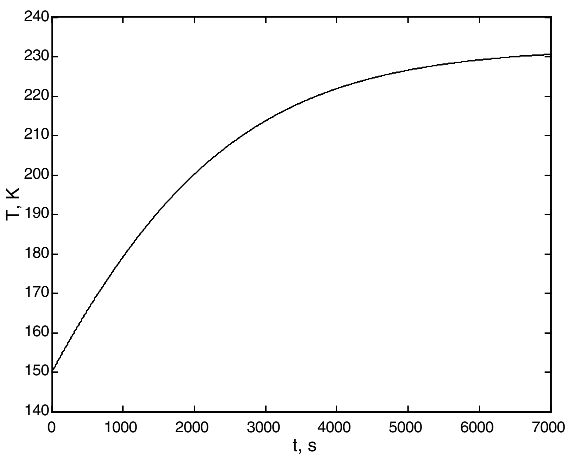

Fig. 2. Numerical solution for the case with radiation and conduction heat loss.

From Fig. 2 one can deduce the time constant and the steady state temperature. It can be seen that the time constant has not changed too much and is about 80 min, but the steady state temperature with respect to the initial value has decreased, to 230 K.

The simple thermal analysis performed in this section shows the importance of different processes (heat source, loss of heat by radiation and conduction, the role of multiple reflections) on the final steady-state temperature of the boards. It illustrates also the fact that an accurate solution can only be obtained when all physical, geometrical and material factors are properly taken into account.

3. Description of the model

The shape of the whole MUPUS penetrator system (i.e. inserting device and the penetrating rod) has been generated in the CAD format from the blueprint drawings of all parts. The model is simplified by neglecting chamfering and rounding smaller than 2 mm. The screw joints are not taken into account. If the neighboring parts are made of the same material and are fixed by screws, they are considered as a single element. The whole model consists of 43 bodies with 1363 surfaces in total. The model has been then imported to ANSYS 8.0 and subsequently adjusted to this FEM program requirement. In particular, the contact surfaces of bodies have been overlapped by the glue command. The model is complemented with material characteristics of MUPUS elements (bodies), such as density, thermal conductivity and specific heat. Altogether 15 different materials are considered, many of them specific for space applications (e.g. titanium alloy IM1318, Delrin, Vespel SP1 and EX 15-15). Tabular values of typical materials or technical specifications of purchased ones are used [2,3]. Meshing of the model has been performed by ANSYS in compliance with the user request that the edges of elements in a thin wall are not longer than the doubled wall width. As the result the model comprised 152,359 finite elements and 48,056 nodes.

The radiation boundary conditions have been set on all external surfaces (i.e. on the penetrator and the insertion device housing), on the internal part of housing that surrounds the electronic box and on all electronic boards [4]. The source term corresponding to heat generation has been applied as a body load to all three electronic boards, giving about 0.45–0.5 W at each board and 1.33–1.5 W in total. The important parameter in the radiative heat transfer to be set in the model is so called external temperature. It corresponds to an ambient medium that exchanges radiation with the elements of the model and was taken to be 100 K in the standard case. As the result of the model definition, the heat is exchanged via radiation among the electronic boards, the internal surface of the housing, and the internal ambient temperature, a parameter that is relevant when the considered radiating bodies are not perfectly black. In that case the radiation is multiply reflected from the boundaries, which the ANSYS program cannot directly account for. The way out of this problem is to introduce the mentioned internal ambient temperature [5]. The radiation is also exchanged between the external parts of MUPUS and the ambient medium surrounding the whole probe. The connected parts transport the heat by conduction. The emission and absorption coefficients of gold have been taken from [4] as equal $\varepsilon = 0.023$ and $\alpha = 0.299$, respectively. The first one describes the emission from the hotter external housing surface to the cooler medium; the second one corresponds to the absorption of heat that is emitted by the warm electronics on the (cooler) internal surface of the housing. Since the radiation transfer is a strongly nonlinear phenomenon ($f \sim T^4$), ANSYS uses the surface mesh independently in two passes, once to solve the linear heat conduction problem and then to deal with the radiative transfer. The program solves iteratively such a coupled problem [7].

The most uncertain value in the modeling is the emissivity of electronic boards. It is so due to heterogeneity of the boards and unknown type of material, from which the electronic elements have been made. Therefore, we have decided to consider the emissivity as a free parameter in the model to be determined from the fit of the calculated temperature variation to experimental data [1]. The thermal conductivity of the boards has been taken as equal to 8 W/m K—an estimated weighted average of metallic and plastic elements on the board. Similarly, the specific heat has been assumed to be 800 J/kg K, in the standard model. It has been found that reasonable changes of those values do not influence significantly the temperature variation with time. Two other parameters that need to be determined in the modeling are (i) the internal ambient temperature that could possibly increase during the heating of the boards, and (ii) the loss of heat through the harness connecting the electronics with the sensors. The second effect was initially neglected in the modeling; i.e. it was assumed that no heat is lost through the cables. Later on, the model was improved to include the heat conduction through the wires driven by the temperature difference between the (hot) electronics and the (cold) penetrator.

4. Results

The experimental data have been taken from the tests performed in the vacuum-thermal chamber on the MUPUS engineering model [1]. The tests comprised eight cycles of chamber temperature variations from about 100 K to more than 300 K. In the cold phase, mechanical tests of MUPUS device were performed after heating the electronics to the minimum accepted temperature of about 220 K. In order to test the thermal properties of the MUPUS device the heating process was allowed to run for much longer time than it was necessary to reach this critical temperature. Altogether 5 heating runs were recorded and the three best ones are compared with our modeling results. Usually, the starting temperature of the electronic board, that contained the temperature sensor, was about 140–150 K. The final temperature that was reached after about 1 h of heating was about 270 K. Several temperature sensors (PT100) were attached to different parts of the device and recorded the temperature variations on its external elements.

The free parameters of the model have been chosen to reproduce the experimental results in the best possible way. Although no formal fitting method has been applied, the final results justify such a simplistic approach. The main lessons learned from the attempted fitting concerns physics of the heat exchange in a complicated system rather than mathematical estimates of the quality of the fit. Such rigorous approach was nevertheless excluded because of high computational costs (a single run takes about 6 h of CPU on PC Pentium IV 2.2 GHz).

The first effect to be investigated is the amount of heat generated in the electronic box. The range of considered values is 1.33–1.5 W. In Fig. 3, we present the results of modeling for those two cases (solid line for 1.5 W, dashed one for 1.33 W) together with the measured temperatures (dash-three dotted line). Although both model curves are two steep in their initial part and two flat in the end, it is obvious that the correct heating power is 1.33 W rather than 1.5 W. An attempt to model better

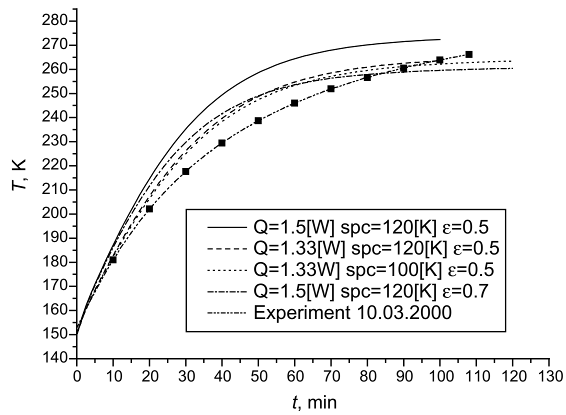

Fig. 3. Temperature variation of the electronic board for different models. The parameters are: Q—applied power, spc—internal space temperature, ε—emissivity of the board. The experimental curve with boxes is given for reference.

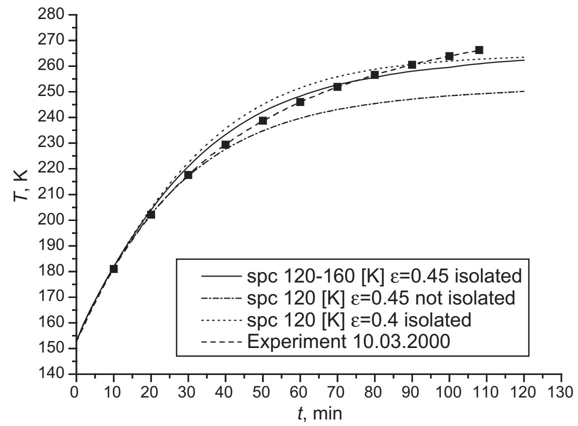

Fig. 4. Temperature variation of the electronic board for different models. The parameters are: spc—internal space temperature, ε—emissivity of the board. The wires are covered or not by teflon insulation.

the curvature of the calculated temperature profiles by changing either the emissivity of the electronic boards, from 0.5 to 0.7 (dash-dotted line), or the internal space temperature, from 120 K to 100 K (dotted line) has not been successful.

In the next set of models, we have tried to include the previously neglected effects: the role of harness connecting the electronic box with the penetrator in heat transfer, and the influence of the varying in time internal space temperature (Fig. 4). The dash-dotted line corresponds to the case of copper wires that are not covered by teflon insulation. Although the first part of the curve approximates the measured results very well, it underestimates the final temperature by about 10 K. The obvious change in the model was to introduce the teflon coating that covers the wires, in agreement with the harness used in the instrument (dotted line) and to slightly decrease its emissivity (from 0.45 to 0.4). The final refinement has been to allow the internal space temperature to increase continuously, so that it lags about 10 K behind the temperature of the wall of housing. The solid line in Fig. 4 that corresponds to this case does not differ by more than 5 K from the experimental curve, a quite satisfactory results considering all unknowns in the model.

The last and fine tuning (Fig. 5) of the model is to extend the range of internal temperature variation to 120–175 K (solid line), which improves significantly the fit in the end phase of the experiment, and to change the specific heat of the boards from 800 to 950 J/kg K (dashed line). Now, the agreement between the model and the experiment can be considered as a very good one; the

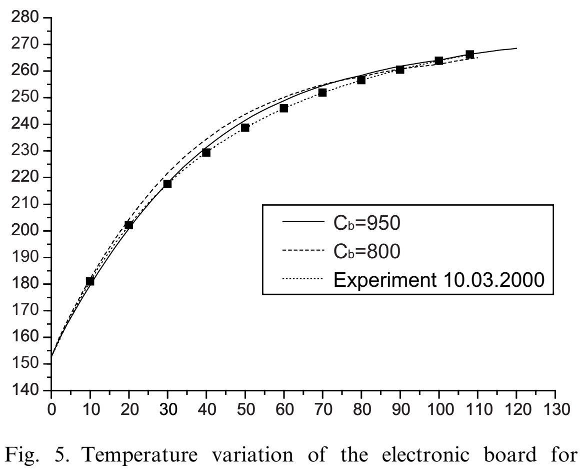

Fig. 5. Temperature variation of the electronic board for different models. The parameters are: C_b—specific heat of the board.

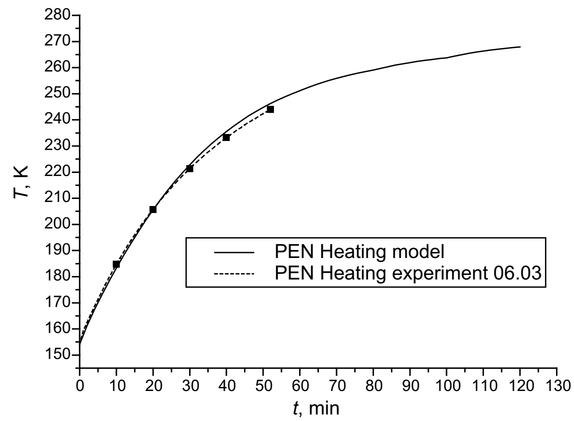

Fig. 6. Comparison of the modeled and experimental temperature variation. The vacuum-thermal experiment took place on 06.03.2000.

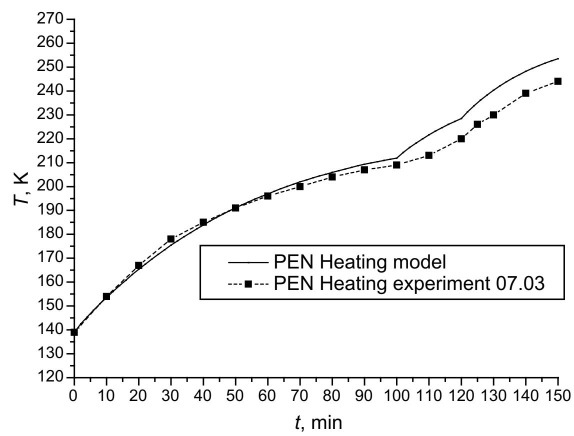

Fig. 7. Comparison of the modeled and experimental temperature variation. The vacuum-thermal experiment took place on 07.03.2000.

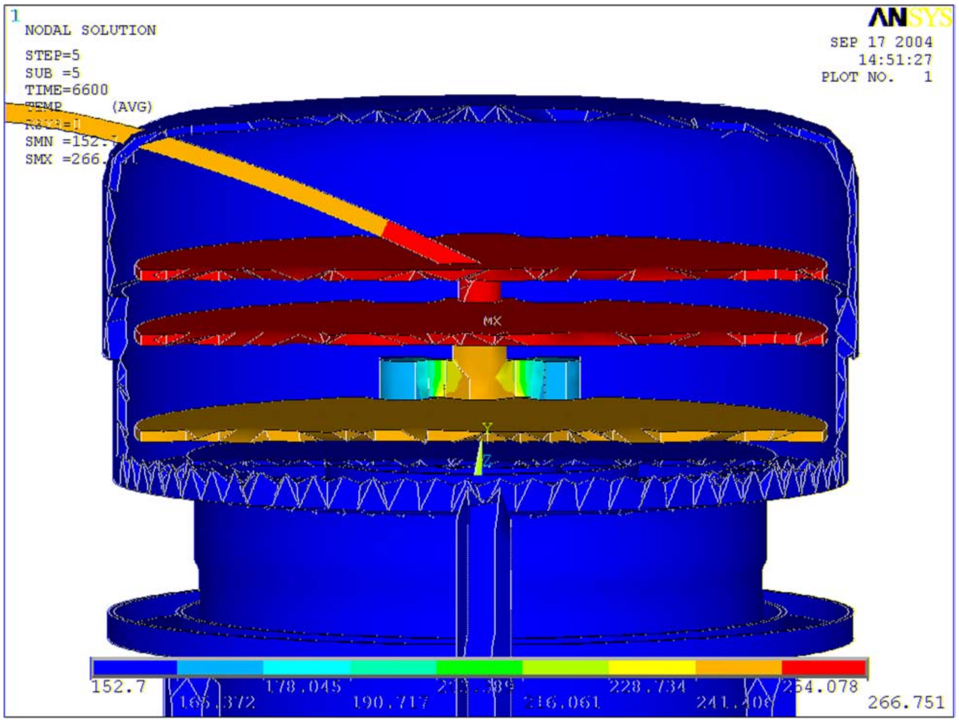

Fig. 8. Temperature distribution in the PEN EL compartment of the MUPUS insertion device.

temperature difference between those two curves does not exceed 3 K. Since the accuracy of temperature measurements is of about ±1 K, there is no need of attempting additional optimization.

Having succeeded in determining the important physical parameters of the model for one experimental curve, we have tried to employ the model with now fixed values of the parameters to other experimental cases (Figs. 6 and 7). The first case shows a very good agreement. The second one refers to the heating with variable power applied (first with 0.66 W, then with 1 W, finally with 1.33 W). Here, the model describes very well the first stretch. Although in the second part of experiment the temperature is qualitatively reproduced by the model, it lies systematically above the measured values. We attribute this effect to a relatively long procedure of switching the power from one value to another, during which the power is not supplied at all.

The advantage of numerical modeling is, of course, a possibility of obtain the temperature field in the whole volume of the analyzed body at any time? See Electronic Annex 1 in the online version of this article. The most interesting however is the stationary state of the device. It is reached after a long time, necessary to equilibrate the heat source (heater) with the sink (radiator). As one could see from the plots (Figs. 3–7) even 100 min. is not enough to get the equilibrium. Nevertheless, the solution obtained for that time should not be significantly different from the stationary state. In Fig. 8 the temperature distribution in the MUPUS insertion device that is reached after 110 min from switching on the heaters, is presented.

One can see three interesting effect. First, the temperature decreases steeply along the harness (the cable from the electronic box to the penetrator). Second the membrane effectively insulates the penetrator from the warm electronic box. Therefore, one should not be concerned about thermal perturbations from the electronics on temperature sensors inside the tube.

5. Discussion

The results of detailed and comprehensive numerical modeling have showed that it is possible, although it is time consuming and cumbersome, to fit quite well the temperature obtained from the model with the measured in a vacuum-thermal chamber. The fitting required determining of many parameters that have not been known a priori with a sufficient accuracy. In that way, the presented approach could be considered as a primitive but efficient version of parameters retrieval procedure. The main factors that determine the thermal behavior of the system are: (i) the value of emissivity of electronic boards ε, (ii) the time-dependent (increasing) internal space temperature that describe multiple

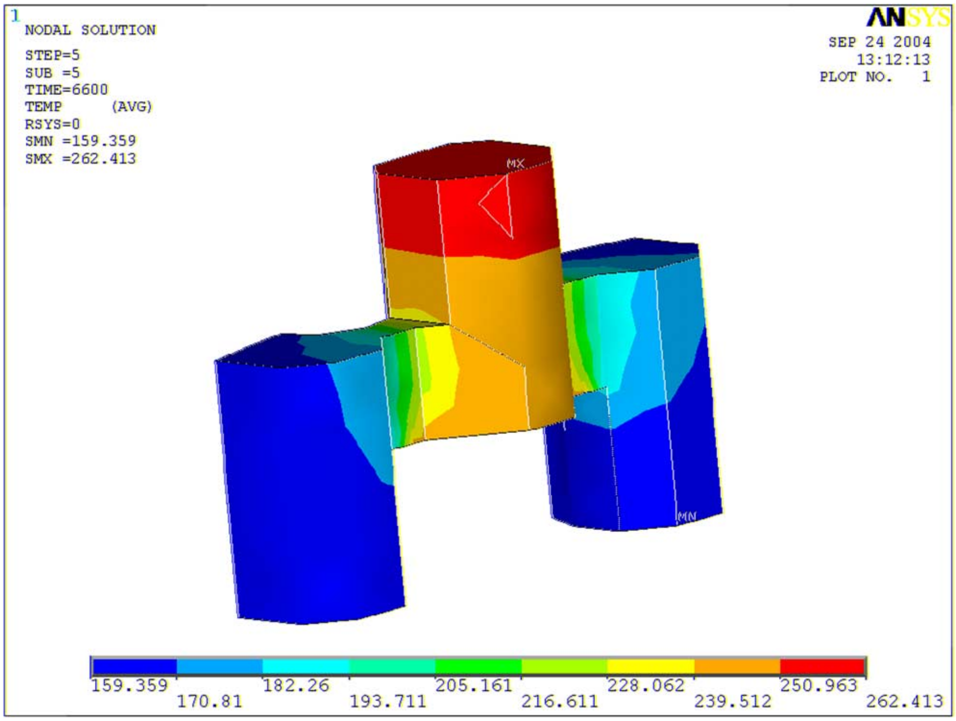

Fig. 9. Temperature distribution in the delrin insulating stand.

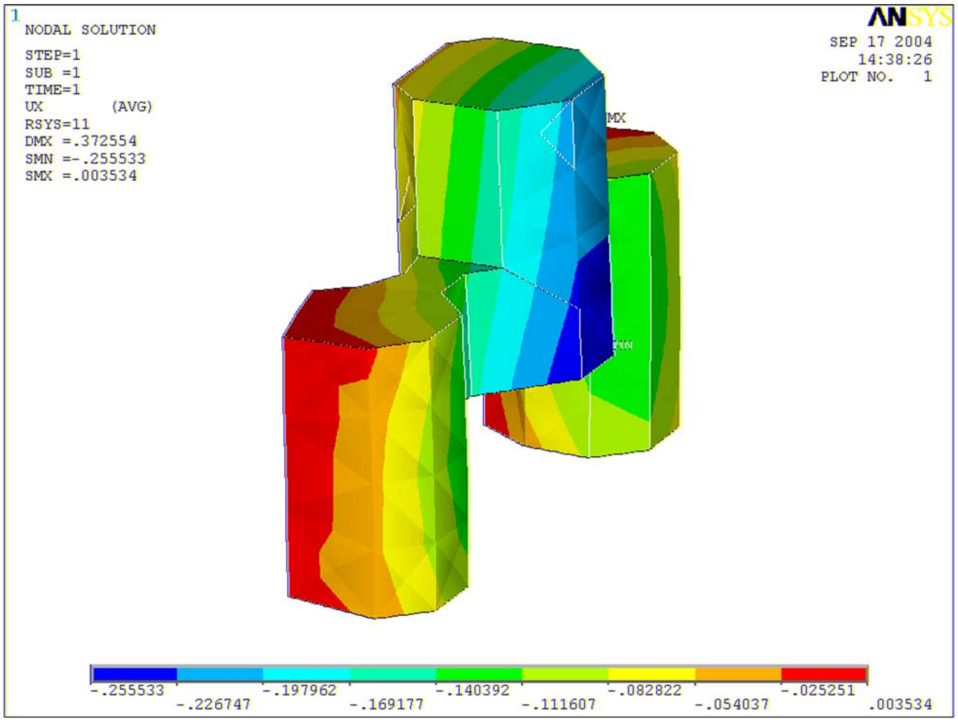

Fig. 10. Elongation of delrin insulating stand in radial direction.

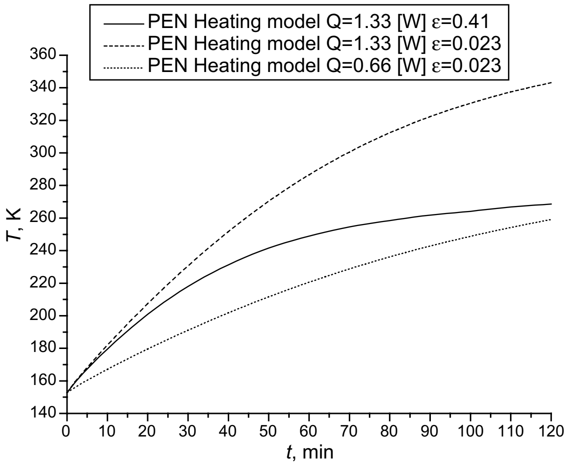

Fig. 11. Temperature variation of electronic board sandwiched by golden foil. The parameters are: Q—applied power, ε—emissivity of the board.

reflection effect, $T_{is} = T^0_{is} + \gamma t$, (iii) the heat conduction along the harness. The minor although important effect includes thermal conductivity K_b and specific heat C_b of the boards. Concluding, if one would like to apply an inversion method to get the best fit one should introduce a number of parameters to be derived: ε, γ, K_b, C_b. The sensitivity of the solution the mention parameters can be estimated from the plot presented in Section 3. The modeling has revealed the interesting aspect of the heat transfer and thermal balance in the box of electronics. The delrin stand acts as efficient heat insulation: the temperature drops by 100 K from the warm to the cold side of the stand. It is shown in Fig. 9.

When the temperature distribution of the stand and the thermal expansion coefficient of delrin (122×10^{-6} K^{-1}) are known, one can obtain the elongation and stresses in the body, that are caused by thermal expansion. Numerical calculations demonstrate that the stand extends radially toward center by 0.25 mm (Fig. 10) for the temperature distribution from Fig. 9.

Another issue that has been clarified in modeling is how to obtain the highest possible temperature of electronics for a given power applied. It appears that golden foil sandwiching the board could give a temperature increase of about 70 K (Fig. 11). Although the ending temperature of about 320 K is too high for the electronics and should be avoided, it seems that proposed solution could spare either applied power or heating time. It should definitely be considered in the future construction of this kind.

It is interesting to compare the results of the final, comprehensive and refined model with the simple analytical approach used in Section 2. The time constant of about 80 min obtained from the (integral) balance equation (5) is not too different from the value of 80–90 min that could be derived from the curve in Fig. 5. The temperature increase obtained in the simple model is too small (90 K instead of 120 K), but this can be understood taking into account all approximations leading to the simple formula (5). Summarizing, the value of approximated analytical solutions consists in a first order assessment of expected results. However, the detailed description of thermal behavior of the considered unit can only be obtained with the advanced numerical model.

Acknowledgement

The authors are very grateful to W. Marczewski and K. Seiferlin for numerous discussions about the subject. The calculations have been performed in the Academic computer center Cyfronet AGH under the grant MNiI/H_I_SD/CBKPAN/002/2004. The paper was partially supported from the KBN project no 5 T121E 027 25.

Appendix A. Supplementary data

Supplementary data associated with this article can be found, in the online version, at doi:10.1016/j.ijheatmasstransfer.2005.04.003.

References

[1] M. Banaszkiewicz, K. Seiferlin, EQM MUPUS PEN Vacuum-thermal Test Report RO-LMU-TR-002/EQM-VT-PEN Iss. 1 04.04.2000.
[2] Thermal and physical properties of titanium and aluminum alloy are obtained from http://www.efunda.com.
[3] Thermal and physical properties of other materials (i.e. delrin, vespel, etc.) are obtained from http://www.goodfellow.com.
[4] A. Panetti, Thermal, in: J.R. Wertz, W.J. Larson (Eds.), Space Mission Analysis and Design, third ed., Microcosm Press, El Segundo, California, 1999, pp. 428–459.
[5] R. Siegel, J.R. Howell, Thermal Radiation Heat Transfer, McGraw-Hill Book Co., New York, 1972, pp. 235–277.
[6] I.M. Ryzhik, I.S. Gradstein, Tables of Integrals, Sums, Series and Products, Academic Press, New York, 1966.
[7] Ansys Release 8.0 Documentation, SAS IP Inc, 2003.